



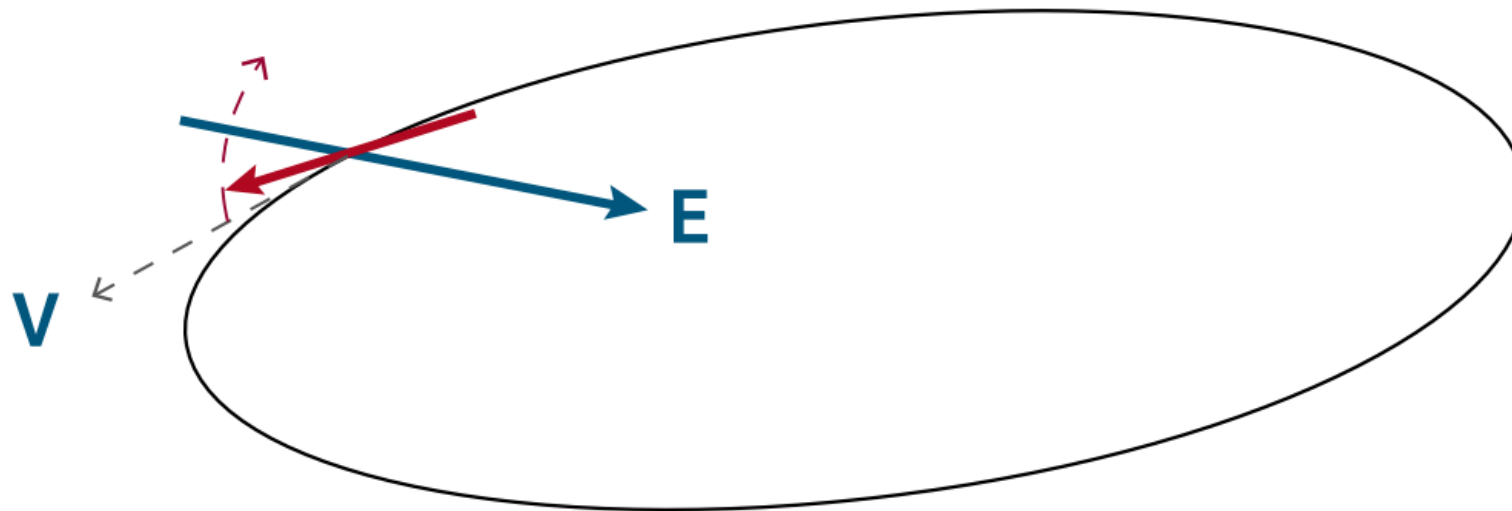
# Search for the Optimal Spin Decoherence Effect in a QFS Lattice

E. Valetov (MSU, USA), Yu. Senichev (FZJ, Germany), M. Berz (MSU, USA)

On behalf of the JEDI Collaboration

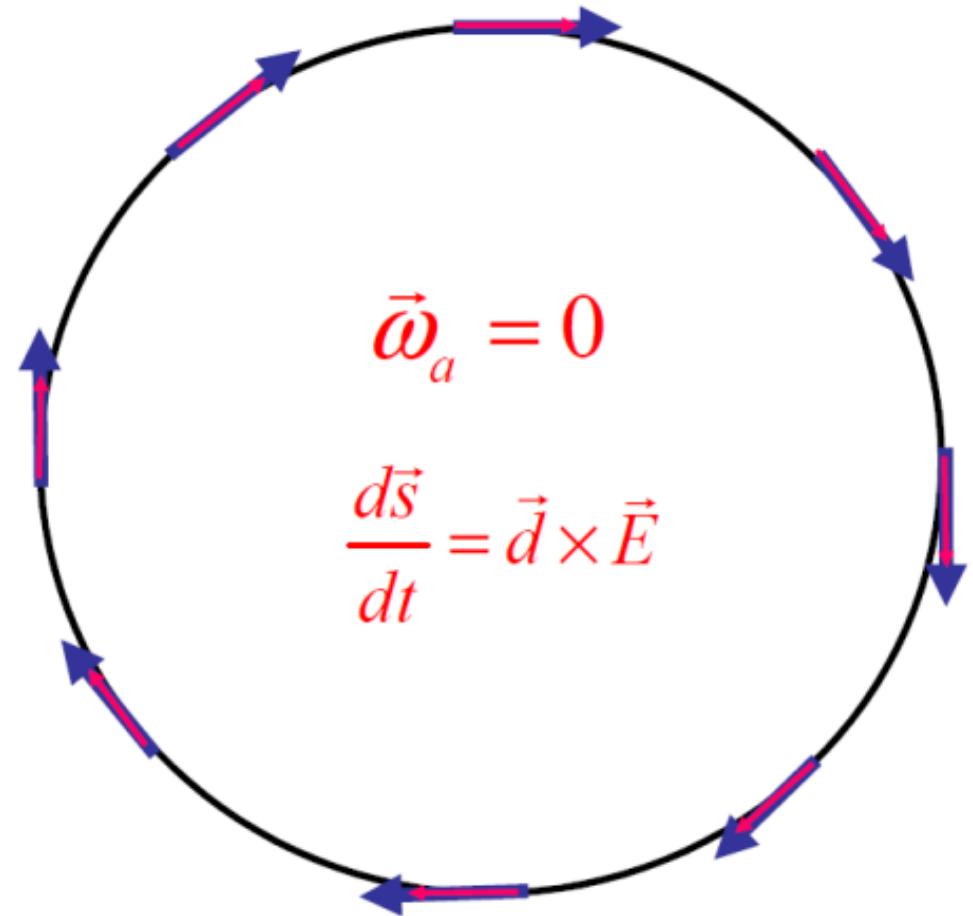
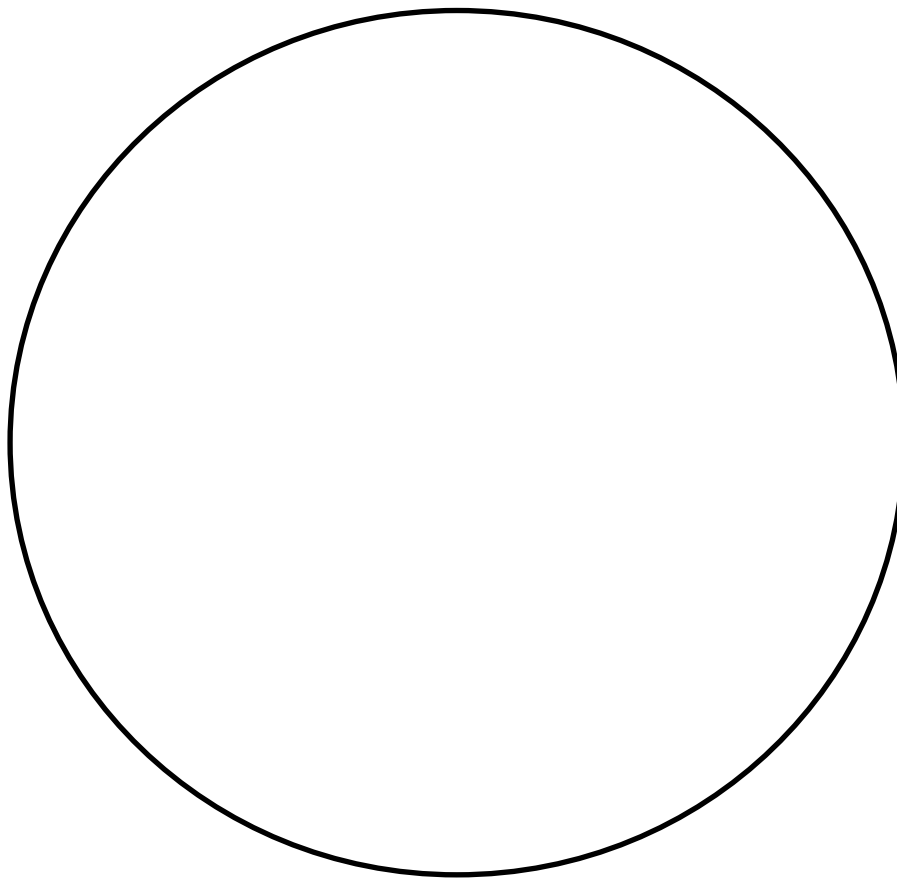
05-Oct-2015

Particle spin alignment along momentum (*frozen spin*)



Radial E-field: torque on spin – rotation out of ring plane

Left: a polarized charged particle (beam) in a storage ring



Right: fixing the horizontal spin along the momentum direction

# Introduction

## Quasi-Frozen Spin (QFS) Technique

Thomas-BMT equation

$$\frac{d\vec{S}}{dt} = \vec{S} \times (\vec{\Omega}_{MDM} + \vec{\Omega}_{EDM})$$

where

$$\vec{\Omega}_{MDM} = \frac{e}{m} \left[ G\vec{B} - \left( G - \frac{1}{\gamma^2 - 1} \right) \frac{\vec{E} \times \beta}{c} \right]$$
$$\vec{\Omega}_{EDM} = \frac{e}{m} \frac{\eta}{2} \left[ \frac{\vec{E}}{c} + \beta \times \vec{B} \right]$$

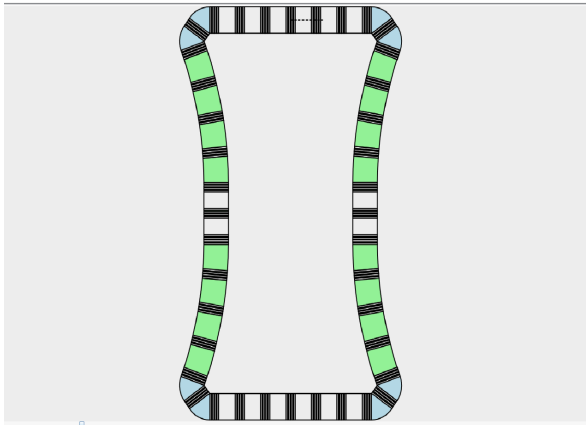
Quasi-Frozen Spin condition

$$\gamma G \Phi_B = \left[ \frac{1}{\gamma} (1 - G) + \gamma G \right] \Phi_E$$

where  $\Phi_B$  and  $\Phi_E$  are the angles of momentum rotation in magnetic and electric bend parts of the ring correspondingly.

# QFS Lattices

## Codename “Senichev 6” Lattice



### Lattice parameters

Length: 16667 cm

Particles: deuterons

Kinetic energy: 270 MeV

*Lattice reference: Yu. Senichev et al., “Quasi-Frozen Spin Method for EDM Deuteron Search”, Proceedings of IPAC’2015, Richmond, VA (2015).*

### Lattice structure

- 4 straight sections (light grey)
- 4 magnetic sections (blue)
- 4 electrostatic sections (green)

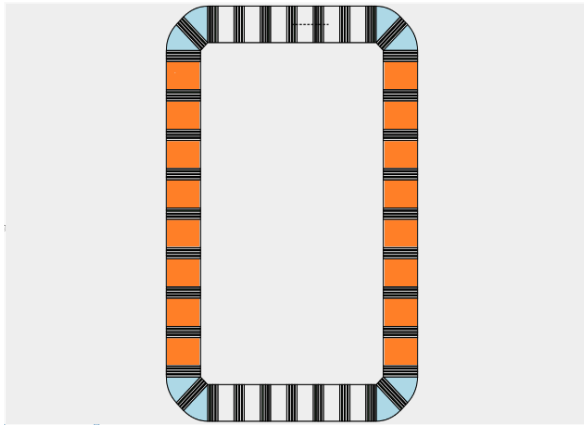
### Decoherence order suppression

- RF cavity: 1<sup>st</sup> and partially 2<sup>nd</sup> order
  - ❖ by mixing the particles relatively to the average field strength, and therefore, averaging out  $\Delta\gamma G$  for each particle

- Sextupoles: remaining 2<sup>nd</sup> order component
  - ❖ which is due to average of  $\Delta\gamma G$  being different for each particle

# QFS Lattices

## Codename “Senichev E+B” Lattice



### Lattice parameters

Length: 14921 cm

Particles: deuterons

Kinetic energy: 270 MeV

### Lattice structure

- 4 straight sections (light grey)
- 4 magnetic sections (blue)
- 4 E+B sections (orange)

### Decoherence order suppression

- RF cavity: 1<sup>st</sup> and partially 2<sup>nd</sup> order
- Sextupoles: remaining 2<sup>nd</sup> order component

E+B Wien Filter elements are used instead of the electrostatic deflector.

### Purpose:

- remove corresponding nonlinear components
- simplify from engineering perspective

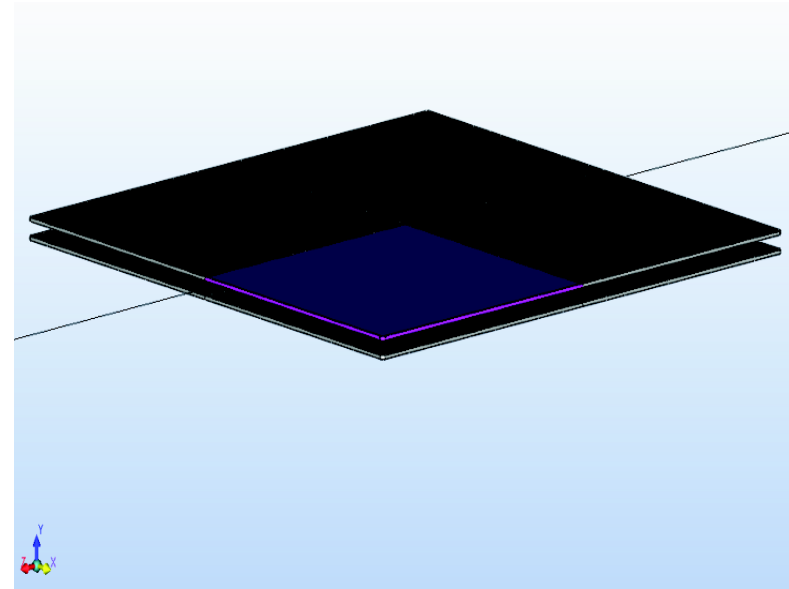
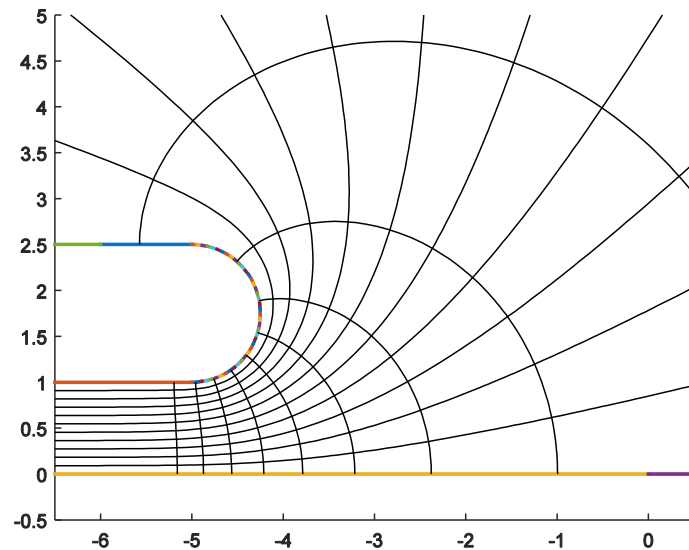
## System analysis

- Analytic relations (quadratic, etc.): see the general character of the system
- Numerical methods (system tracking in *COSY Infinity*): have final understanding of which orders are needed for spin decoherence less than 1 rad in 1000 s / 1 billion turns

## Developed solution

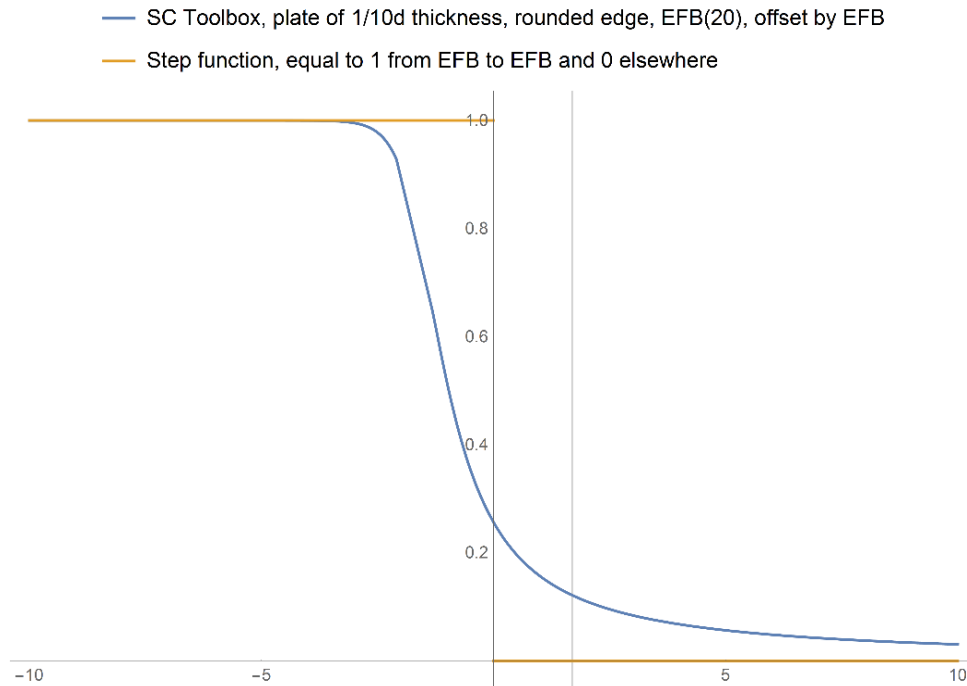
- *COSY Infinity* programs
  - Code for manual and automatic optimization of lattice
    - Choice of three objective functions
    - One differential algebra (DA) objective function
  - Spin tracking code
  - Output data to files for storage and further processing
- *Mathematica* programs
  - Store certain results of *COSY* runs in an organized way
  - Process and QA check that data
  - Generate reports that aggregate processed data in plot and table format

# Fringe Field of the Electrostatic Deflector [4]



- Fringe fields of semi-infinite capacitors with solid metal plates were modeled in *MATLAB* using *Schwarz-Christoffel Toolbox* v.2.3 [5] and analyzed in *Mathematica*.
- Results were compared with those obtained for finite rectangular solid metal capacitors in *Coulomb* by H. Soltner (FZJ, Germany).

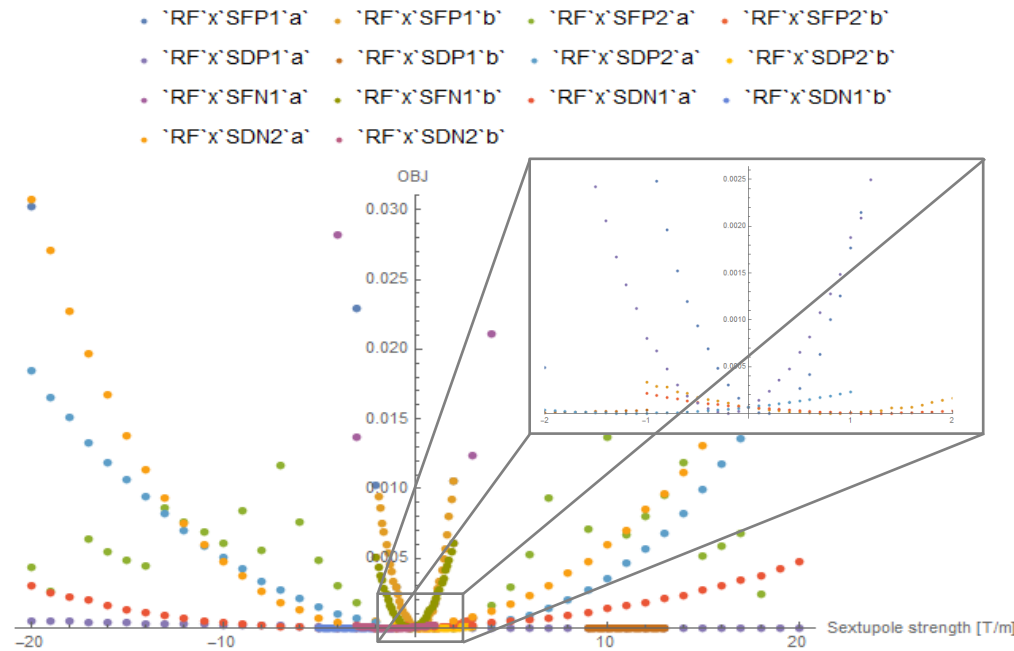




Enge Coefficient	Value
$h_0$	1.0614024399605924
$h_1$	1.6135741290714967
$h_2$	-0.9401447081042862
$h_3$	0.4781500036872176
$h_4$	-0.14379986967718494
$h_5$	0.017831089071215347

“Senichev 6” lattice electrostatic deflector:

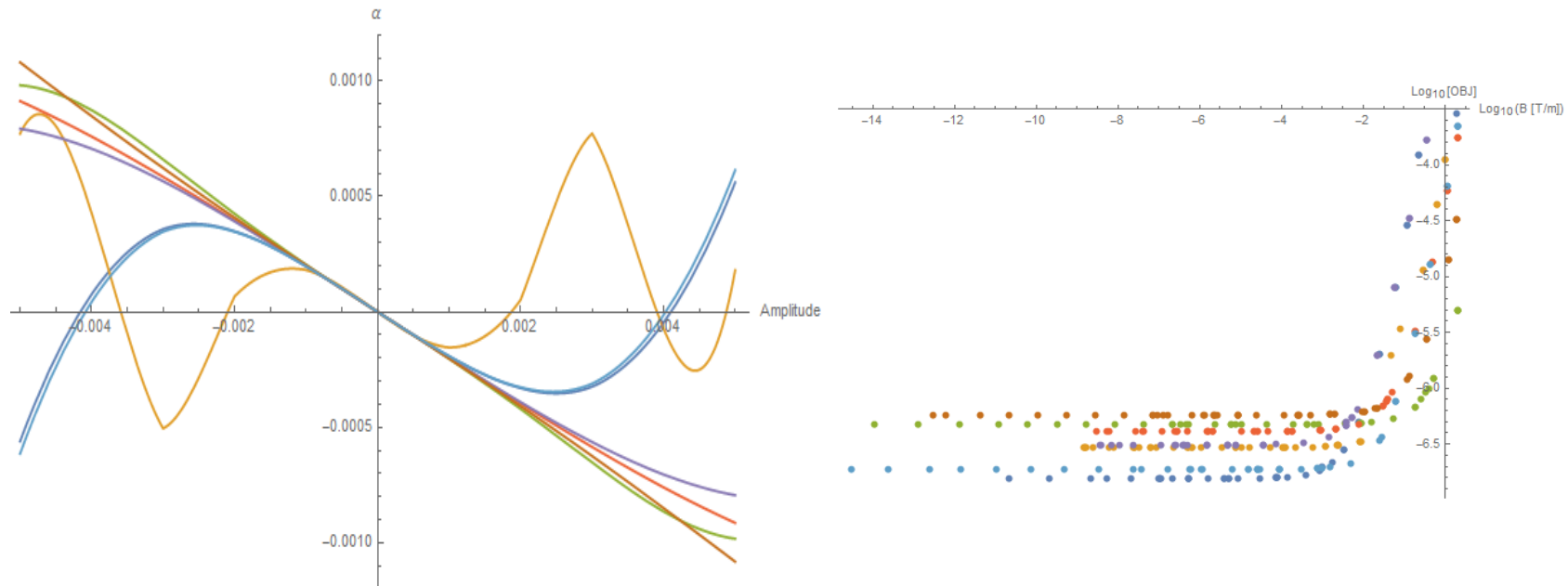
- Semi-infinite capacitor
- Plate thickness 10% of distance between plate and midplane
- Rounded edges



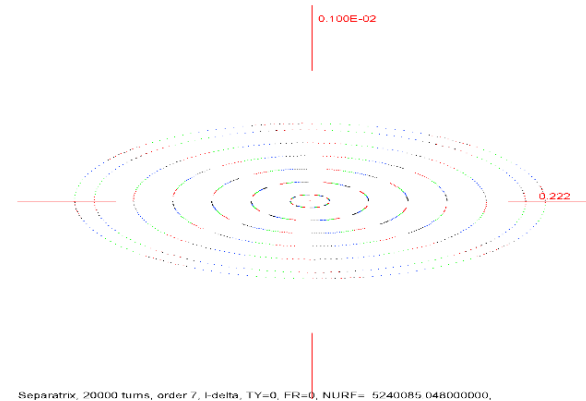
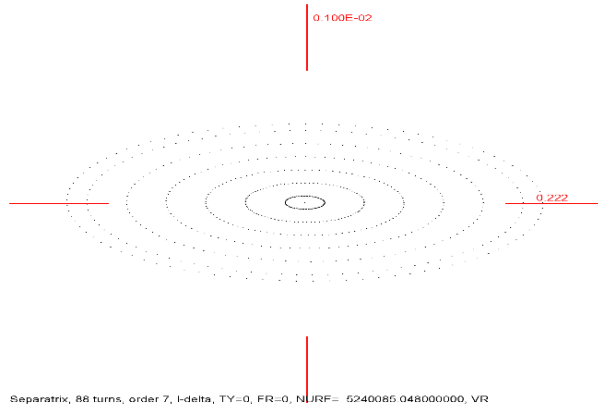
Optimization Context	Optimal Point	OBJ Value
`RF`x`SFP1`a`	0.	0.0000662735
`RF`x`SFP1`b`	0.2	$3.01296 \times 10^{-6}$
`RF`x`SFP2`a`	1.	$9.43392 \times 10^{-6}$
`RF`x`SFP2`b`	0.8	$3.2609 \times 10^{-7}$
`RF`x`SDP1`a`	11.	$8.8197 \times 10^{-7}$
`RF`x`SDP1`b`	10.6	$5.23617 \times 10^{-7}$
`RF`x`SDP2`a`	1.	$4.79843 \times 10^{-6}$
`RF`x`SDP2`b`	1.2	$8.71622 \times 10^{-7}$
`RF`x`SFN1`a`	0.	0.0000662735
`RF`x`SFN1`b`	-0.2	$1.5856 \times 10^{-6}$
`RF`x`SDN1`a`	-3.	$1.03277 \times 10^{-6}$
`RF`x`SDN1`b`	-2.9	$5.88324 \times 10^{-7}$
`RF`x`SDN2`a`	-1.	$2.22602 \times 10^{-6}$
`RF`x`SDN2`b`	-1.2	$3.48314 \times 10^{-7}$

- ❖ 20000 turn spin tracking in  $x - a$ ,  $y - b$ , and  $l - \delta$  planes, RF cavity on/off, various RF cavity frequencies and voltages
- ❖ Objective function represents spin decoherence
- ❖ Each curve shows manual optimization by a sextupole strength
- ❖ Compared with  $x - a$  plane, in  $y - b$  plane
  - ❖ curves are more parabolic
  - ❖ objective function values tend to be lower

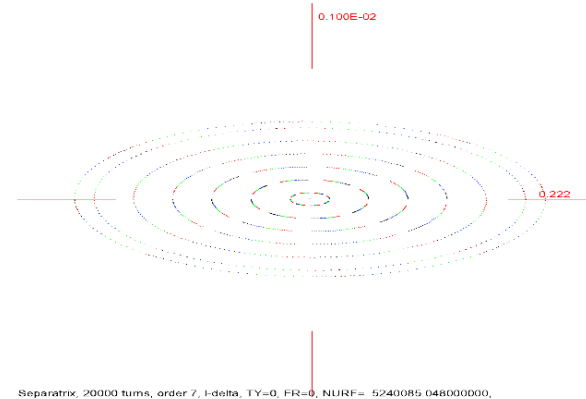
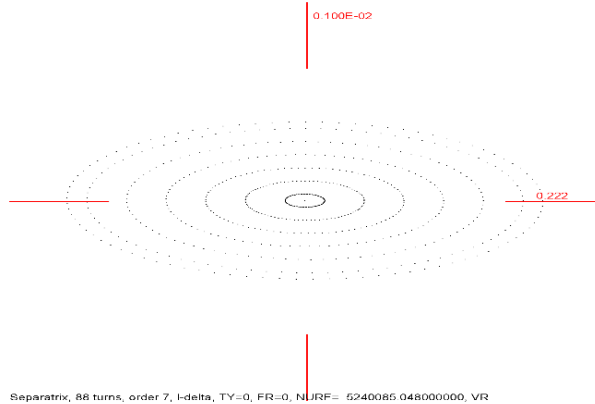
# Automatically optimized sextupole strengths



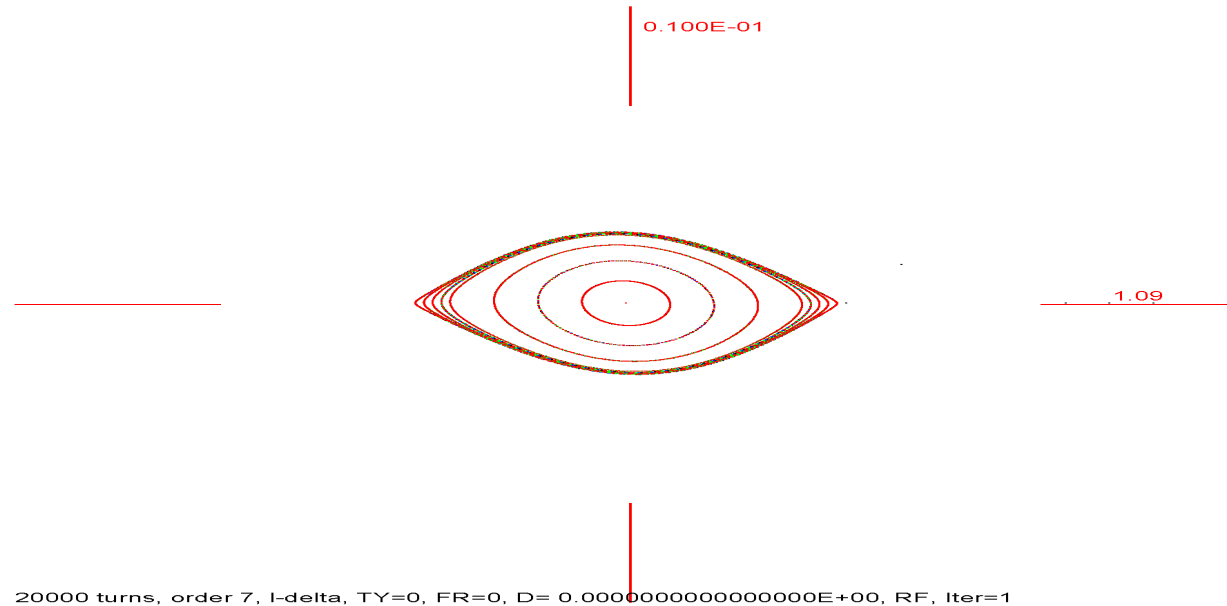
- ❖ Start from manually optimized sextupole strengths values
- ❖ Further optimize them using *LMDIF* optimizer
  - When RF on, curves are typically bounded by symmetric slanted lines
- ❖ On the right plot, the thickness of the optimums is shown on *log – log* scale
  - Considering the accuracy, with which the physical sextupole strengths can be set, the thickness is acceptable



- ❖ Spin decoherence  $\Delta\gamma G$  is order-wise proportional to orbit lengthening  $\Delta l/l$
- ❖ In the example above, RF cavity is set to 5.2 MHz 100kV
- Period particle orbit in  $l - \delta$  plane is approximately 88 turns near ref. particle
- ❖ Therefore, the period of energy averaging  $\Delta\gamma G$  is 88 turns
- ❖ The larger the period of this averaging, the larger the amplitude of oscillations caused by the RF cavity (*cf. infra*)

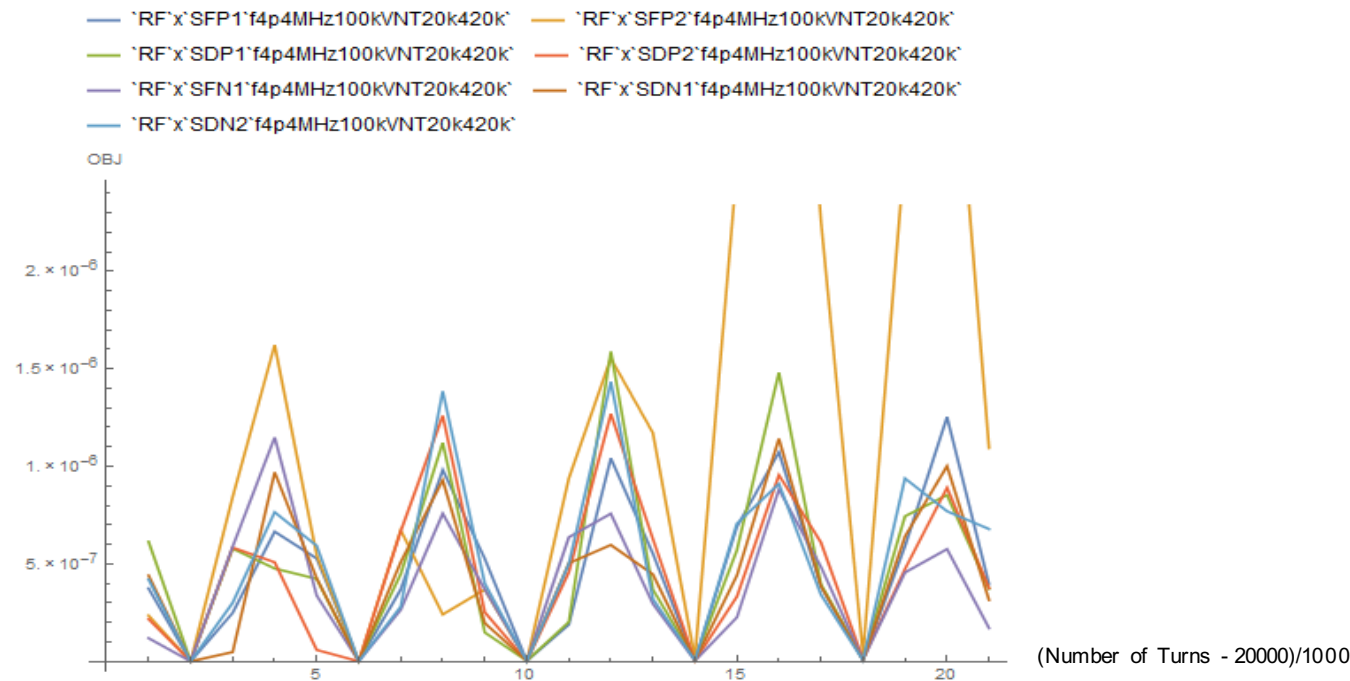


- ❖ W/o RF cavity, spin motion would have a period proportional to  $\Delta\gamma G \sim 10^{-4}$ , where  $\Delta\gamma \sim 10^{-3}$  and  $G = 0.14$
- ❖ For good energy averaging, the order of RF frequency must be 1-2 times higher than  $\Delta\gamma G$
- ❖ RF cavity frequency in the lattice is  $\sim 2$  orders faster  $\Rightarrow$  good energy averaging



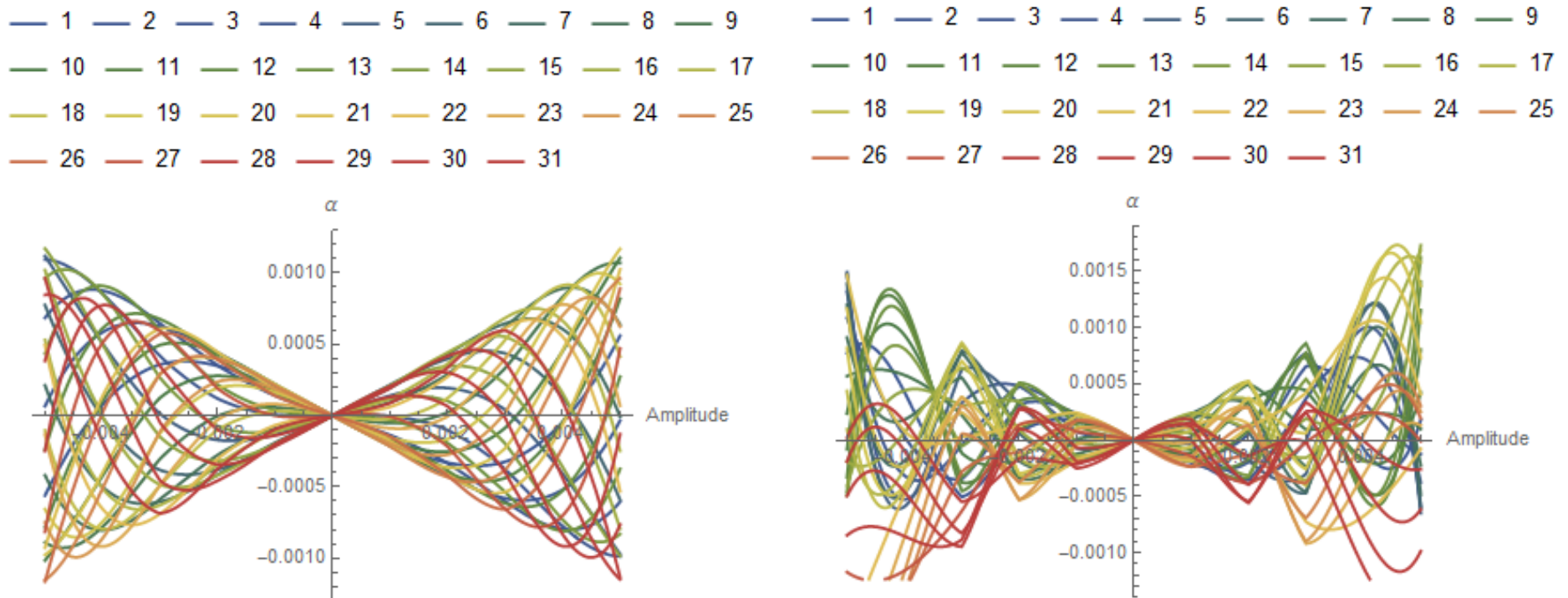
- ❖ 20000 turn spin tracking in  $l - \delta$  plane
- ❖ Separatrix for the motion of particles
- ❖ In the example above, RF cavity is set to 1MHz 50kV
  - Order of  $\delta$ -variance:  $10^{-2}$
  - Size of the separatrix:  $5 \times 10^{-3}$
  - Period of the energy variance averaging: 20 turns
- ❖ Spin precession frequency:  $10^{-4}$
- ❖ Therefore, energy averaging due to RF cavity is  $\sim 2$  orders faster

# Time evolution of spin decoherence measure: “Senichev 6.2” $x - a$ 420k turns (with RF cavity)



- ❖ At 20000 turns, the order of spin decoherence was not sufficiently low to be satisfactory at that point of analysis
- ❖ So we have observed what happens to the objective function as a function of number of turns
- ❖ We plot the objective function against number of turns from 20000 to 420000 turns with the step of 20000
- We note that significant minima occur periodically
- In  $x - a$  and  $y - b$  planes for most sextupole strengths: indication that objective function **remains in the same range**

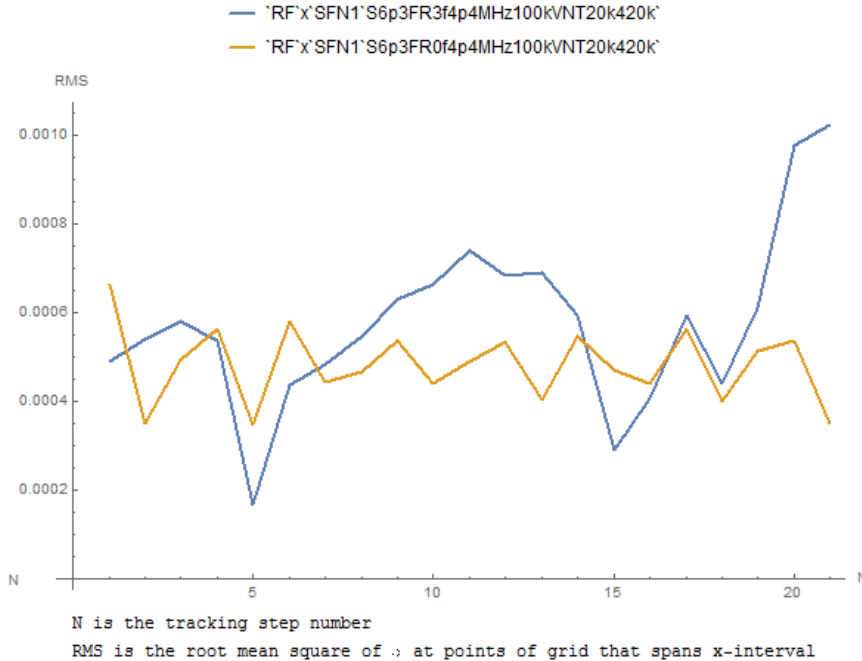
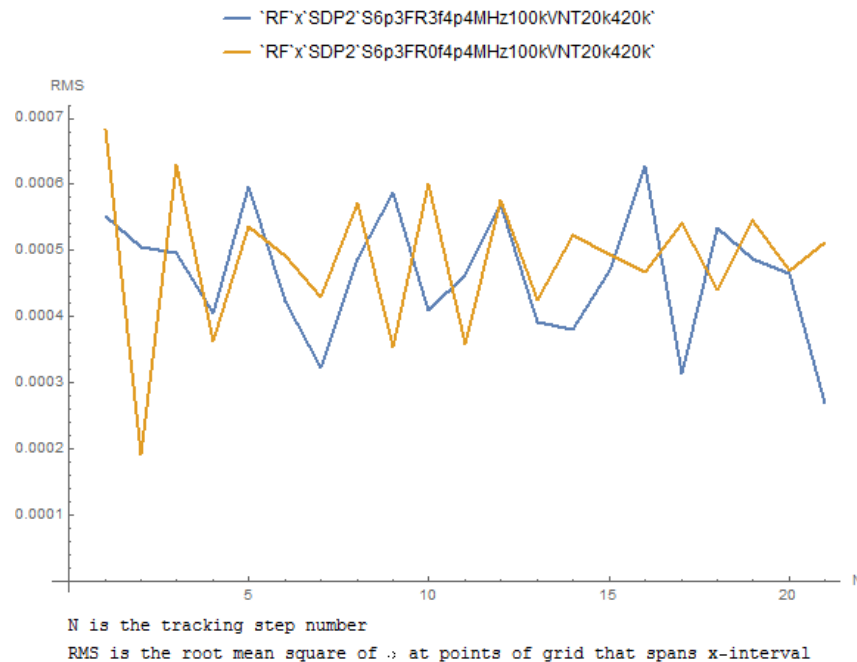
# Time evolution of spin decoherence measure: “Senichev 6.2” $x - a$ 420k turns (with RF cavity)



- ❖ We plot evolution of  $\alpha$ -amplitude plots against number of turns from 20000 to 420000 turns
- For most sextupoles, oscillations seem to be bounded by two slanted lines as seen in the first picture
- Plot for SFP2 was exceptional due to low dispersion at the sextupole
- ❖ This is because RF cavity introduces forced oscillation into the system
- ❖ We could attempt to reduce its amplitude by decreasing RF cavity's voltage and decreasing its frequency by about an order, but we simply deleted SFP2

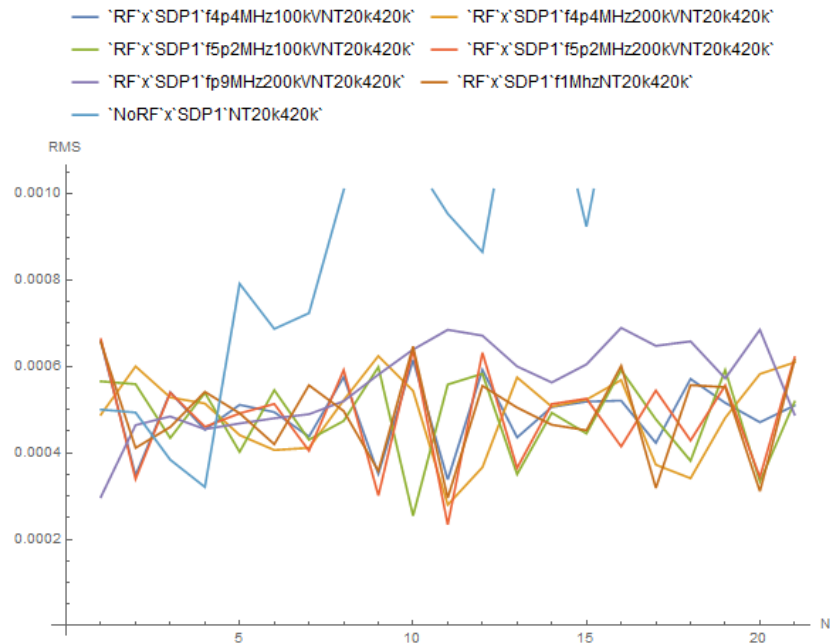


# Time evolution of RMS of spin decoherence: fringe fields vs. no fringe fields

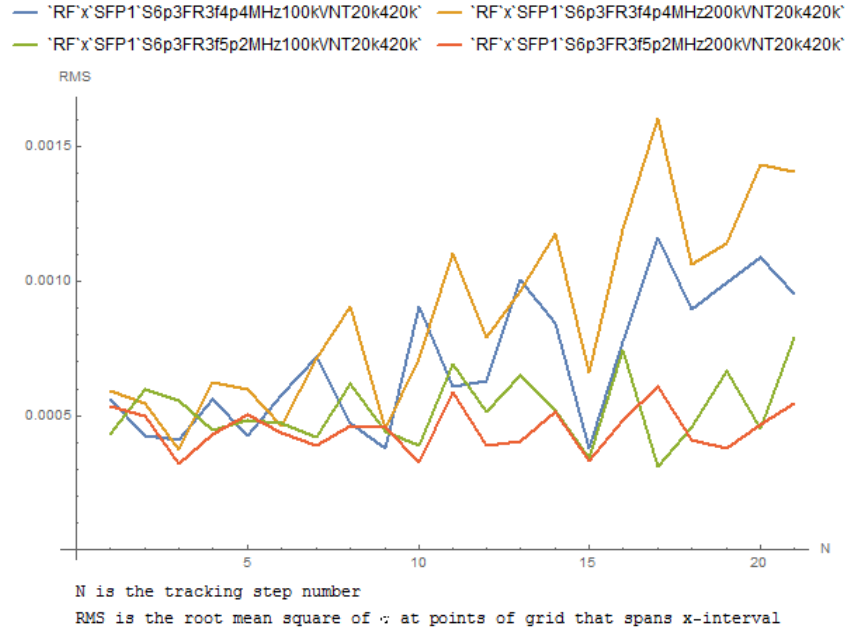


- ❖ Spin decoherence as a function of number of turns is often similar in fringe field modes 0 (no fringe fields) and 3 (most accurate).
- ❖ Sometimes, there is spin decoherence growth in FR 3 but no growth in FR 0.
- ❖ Previous plots were FR 0; starting from this slide we specify FR mode.

# Time evolution of RMS of spin decoherence: “Senichev 6.2” $x - a$ 420k turns



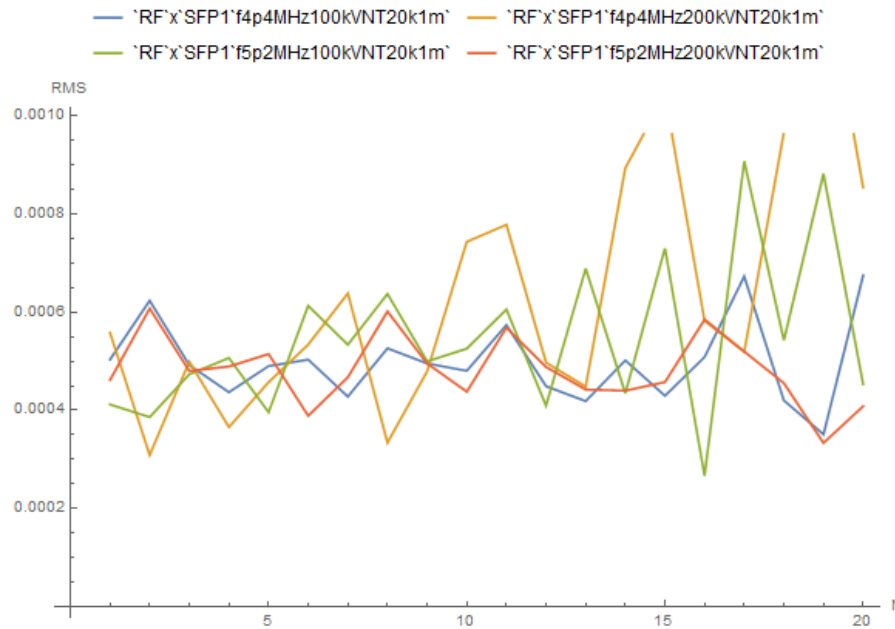
FR 0



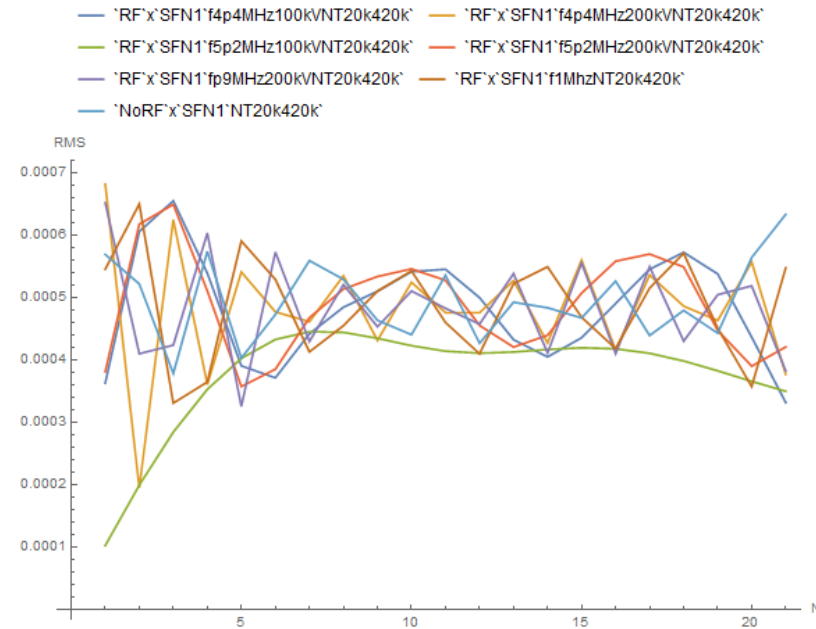
FR 3

- ❖ The RF cavity often limits spin decoherence to a range, at least for the number of turns of the order of  $5 \times 10^5$ .

# Time evolution of RMS of spin decoherence: “Senichev 6.2” $\chi - a$ 1M turns



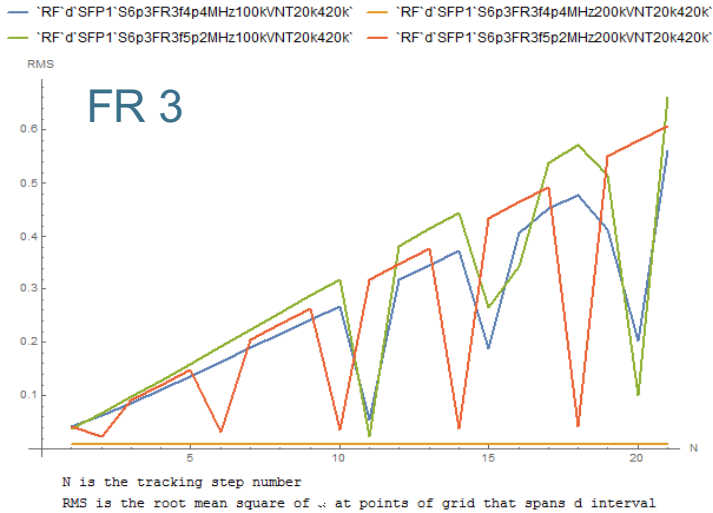
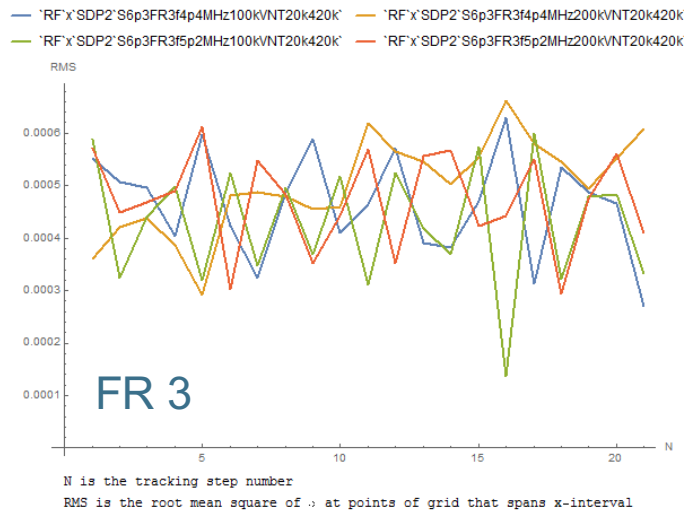
FR 0



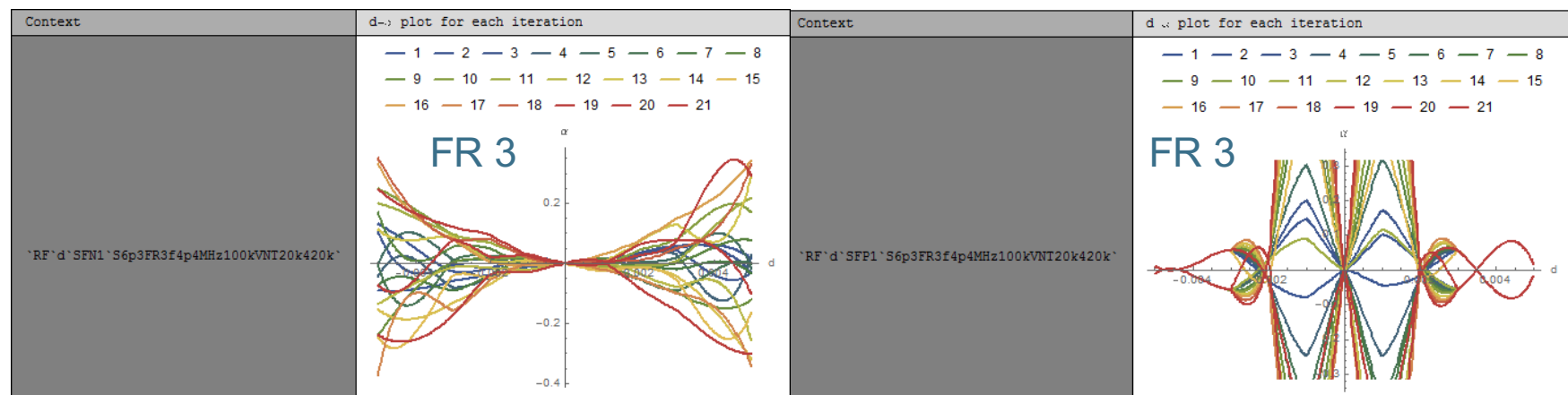
FR 0

- ❖ For some sextupoles and RF cavity settings, spin decoherence goes out of range and starts to increase after  $\sim 10^6$  turns
- ❖ We have to find a set of RF cavity settings, sextupoles, and sextupole settings such that spin decoherence is sufficiently small in all planes, even if there is such an increase

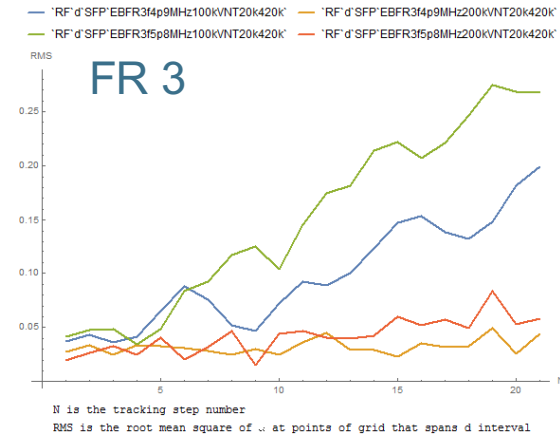
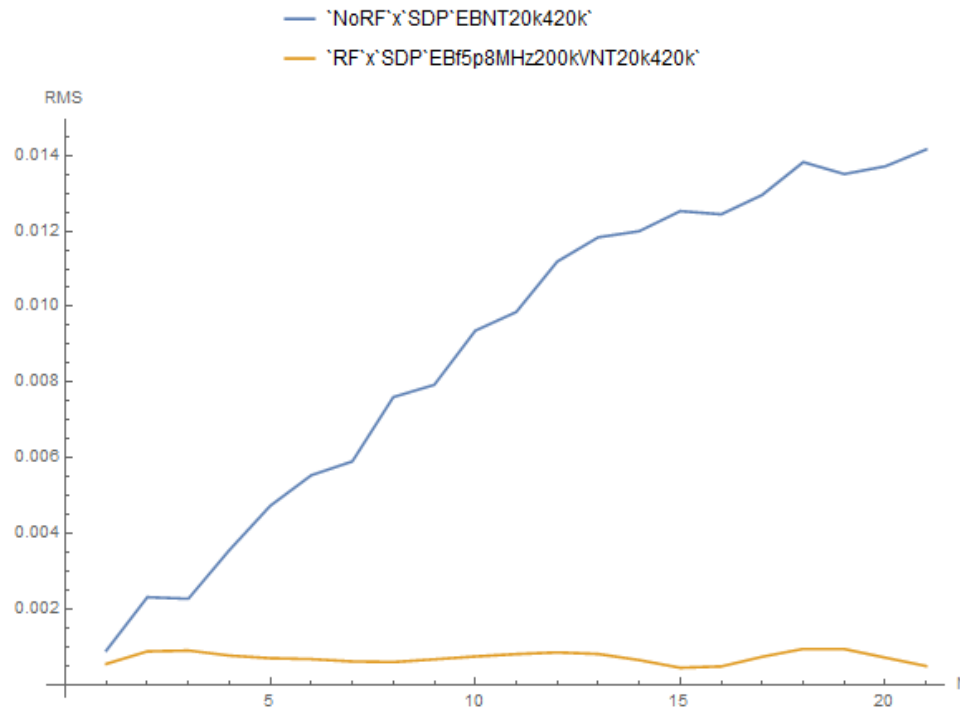
# Time evolution of RMS of spin decoherence: “Senichev 6.2” $l - d$ 420k turns



High nonlinearities introduced by a sextupole family can cause decoherence growth for some RF cavity settings.

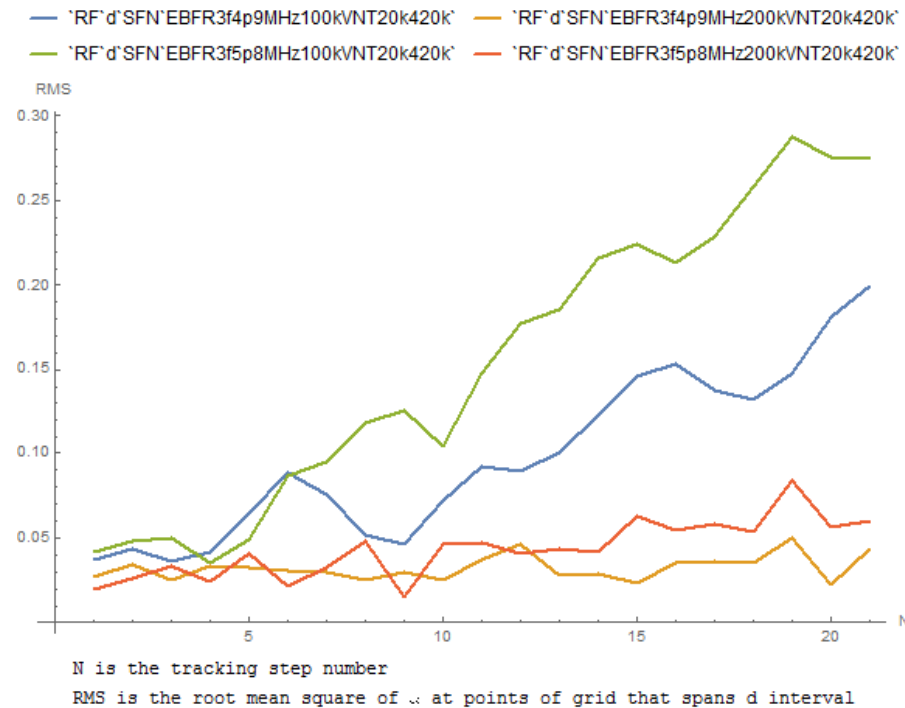


# Time evolution of RMS of spin decoherence: “Senichev E+B” $\chi - a$ 420k turns



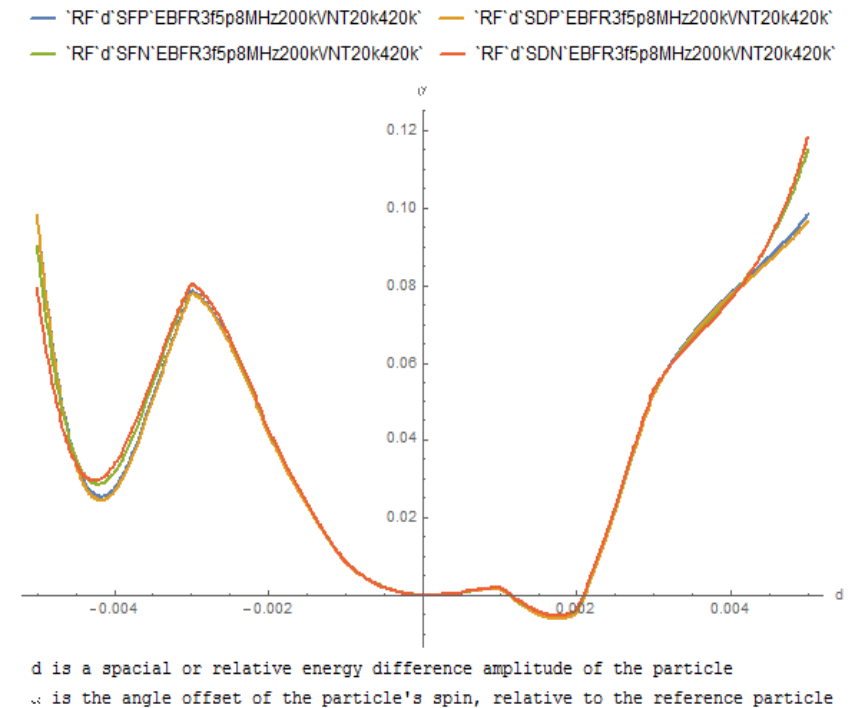
- ❖ Again, the RF limits the spin decoherence to range, at least for the number of turns of the order of  $5 \times 10^5$ .
- ❖ High nonlinearities introduced by a sextupole family can cause decoherence growth for some RF cavity settings.

# Time evolution of RMS of spin decoherence: “Senichev E+B” $l - d$ 420k turns



FR 3

In this case, sextupole family behavior was practically the same.



FR 3

- At present, calculations indicate that the use of RF cavity and sextupoles alone in the considered QFS lattices may be sufficient to optimize the spin decoherence to less than 1 rad in 1 billion turns
- We will continue to work on optimization spin decoherence using the RF cavity and the sextupole strengths in all planes simultaneously
- We will track the obtained solution for a larger number of turns
- We will try to obtain an improved objective function based on tracking of differential algebra (DA) vector-valued particle rays.
- We will try suppressing decoherence using octupoles in addition to sextupoles

- [1] H. Ströher, *Design Study EDM*, Forschungszentrum Jülich, presentation at NuPECC Meeting Edinburgh, October 10, 2014
- [2] Yu. Senichev et al., *Quasi-Frozen Spin Method for EDM Deuteron Search*, Proceedings of IPAC'2015, Richmond, VA, 2015
- [3] Yu. Senichev et al., *Spin Tune Decoherence Effects in Electro- and Magnetostatic Structures*, Proceedings of IPAC'2013, Shanghai, China, 2013.
- [4] E. Valetov and M. Berz, *Calculation of Fringe Fields of Semi-Infinite Electrostatic Deflectors*, preprint of report, Michigan State University, East Lansing, MI, 2015.
- [5] T. Driscoll, *A MATLAB toolbox for Schwarz-Christoffel mapping*, ACM Trans. Math. Softw., 22(2):168-186, June 1996.



